Excitonic photoluminescence in symmetric coupled double quantum wells subject to an external electric field

J. Soubusta,* R. Grill, P. Hlídek, and M. Zvára
Institute of Physics, Charles University, Ke Karlovu 5, 121 16 Prague 2, Czech Republic

L. Smrčka
Institute of Physics, Academy of Science of the Czech Republic, Cukrovarnická 10, 162 53 Prague 6, Czech Republic

S. Malzer, W. Geißelbrecht, and G. H. Döhler
Institut für Technische Physik I, Universität Erlangen-Nürnberg, Erwin-Rommel-Straße 1, 91058 Erlangen, Germany
(Received 22 March 1999)

The effect of an external electric field F on the excitonic photoluminescence (PL) spectra of a symmetric-coupled double quantum well (DQW) is investigated both theoretically and experimentally. We show that the variational method in a two-particle electron-hole wave-function approximation gives a good agreement with measurements of PL on a narrow DQW in a wide interval of F including flat-band regime. The experimental data are presented for a molecular-beam-epitaxy–grown DQW consisting of two 5-nm-wide GaAs wells, separated by a 4-monolayers (ML's)-wide pure AlAs central barrier, and sandwiched between $Ga_{0.7}Al_{0.3}As$ layers. The bias voltage is applied along the growth direction. Spatially direct and indirect excitonic transitions are identified, and the radius of the exciton and squeezing of the exciton in the growth direction are evaluated variationally. The excitonic binding energies, recombination energies, oscillator strengths, and relative intensities of the transitions as functions of the applied field are calculated. Our analysis demonstrates that this simple model is applicable in the case of narrow DQW's, not just for a qualitative description of the PL peak positions but also for the estimation of their individual shapes and intensities. [S0163-1829(99)01532-5]

I. INTRODUCTION

Because of their technical importance and unique physical properties, semiconductor quantum wells have been the subject of intensive research since their first fabrication in 1973. A brief review of the main achievements and a number of representative references can be found, e.g., in Refs. 1 and 2. The tunnel-coupled quantum states in double quantum wells (DQW's) are very sensitive to both electric and magnetic fields, and changes induced by these fields have been intensively studied by photoluminescence (PL), PL excitation, and photoconductivity.[3–8]

A symmetric-coupled DQW consists of two identical quantum wells separated by only a thin barrier. The energy levels of the coupled QW's split owing to the interwell tunneling. In the flat-band condition ($F=0$), the eigenfunctions of the DQW have defined symmetries. In this situation, only transitions between electron and hole states of the same symmetry are optically allowed. The ground-state wave function is symmetric, while that of the first excited state is antisymmetric. When an electric field is applied to the DQW, the wave functions become predominantly localized in one well only. Transitions allowed in the flat-band case evolve into spatially indirect (interwell) transitions, which shift linearly in energy as a function of the applied field. On the other hand, transitions forbidden in the flat-band case become allowed and represent spatially direct (intrawell) transitions. Two factors determine the optical transition intensities: (a) the overlap integral of the electron and hole single-particle wave functions, and (b) the population of the energy subbands for a given temperature. In order to describe the optical transitions correctly, one has to account for the Coulomb interaction between electrons and holes. We use a two-particle wave function composed of the electron and hole single-particle wave functions multiplied by a function of their relative positions to get an exciton binding energy.

The purpose of this paper is to demonstrate that our quite simple theory, applied to the PL results obtained from our specifically designed sample, provides excellent quantitative agreement with regard to both the energetic position of the PL peaks and their shapes and intensities as a function of applied electric fields. These results represent clearly a further improvement compared to the previously reported results.[3,4,6,8]

II. THEORY

The calculation starts from the envelope-function excitonic Hamiltonian

$$H_{ex}=H_{oe}+H_{oh}+H_{2D}+U+E_g, \tag{1}$$

where the respective electron and hole single-particle terms read[1]

$$H_{o\nu}=-\frac{\hbar^2}{2}\frac{\partial}{\partial z_\nu}\frac{1}{m_\nu(z_\nu)}\frac{\partial}{\partial z_\nu}+V_\nu(z_\nu)-q_\nu F z_\nu, \tag{2}$$

$\nu=\{e,h\}$ denotes an electron or hole, and q_ν is the respective charge. $m_\nu(z_\nu)$ and $V_\nu(z_\nu)$ are the respective electron or hole z_ν-dependent effective masses and confining potentials of the DQW structure. The electric field F is applied along the z axis parallel to the growth direction. H_{2D} represents the

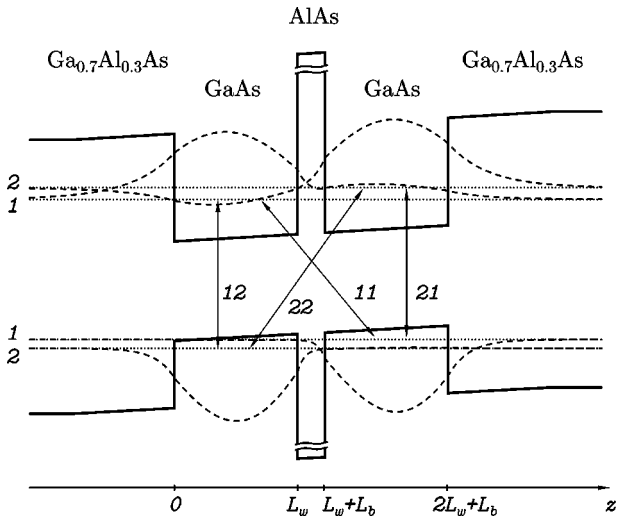

FIG. 1. Scheme of the DQW potential profile with an applied external field (solid lines). The energy levels (dotted lines) and wave functions (dashed lines) of electrons and holes are shown as well. Bases of the wave functions are at the corresponding energies and their amplitudes are plotted in arbitrary units. The plot was calculated for $L_w=5$ nm and $F=30$ kV/cm.

kinetic energy in the xy plane. The electron-hole exciton interaction is included by means of the Coulomb term U, and the GaAs band-gap energy E_g completes the total energy H_{ex}.

Eigenenergies and eigenfunctions of the single-particle one-dimensional Hamiltonian $H_{o\nu}$ are found by using linear combinations of analytical functions $\sin(\xi)$ and $\cos(\xi)$ (wells, $F=0$), Airy functions $\mathrm{Ai}(\xi)$ and $\mathrm{Bi}(\xi)$ (wells, $F>0$), or $\exp(\pm\xi)$ (barriers), and by matching the wave-function amplitudes and their derivatives divided by the effective masses at each interface. Representative results of such a calculation made for a DQW structure with $L_w=18$ ML, $L_b=4$ ML (≈ 5.09 nm and 1.13 nm, respectively), and for $F=30$ kV/cm are schematically plotted in Fig. 1.

The first two single-particle eigenfunctions $\varphi_1^\nu(z_\nu)$, $\varphi_2^\nu(z_\nu)$ of $H_{o\nu}$ are used to construct a set of basis functions for the variational calculation of the exciton states as a single product of one electron and one hole wave function multiplied by a function of relative electron hole positions[4–6]

$$\chi_{ij}=N_{ij}\varphi_i^e(z_e)\varphi_j^h(z_h)\exp\left[-\frac{\sqrt{\rho^2+\alpha_{ij}(z_e-z_h)^2}}{R_{ij}}\right], \quad (3)$$

where the normalization factors N_{ij} and the variational parameters R_{ij},α_{ij} are, in general, different for each exciton. While the z coordinates of both carriers are specified absolutely (z_e,z_h), only the relative distance between them projected onto the xy plane (ρ) is relevant. We minimize the total energy [Eq. (1)] for each exciton separately and obtain four wave functions $\{\chi_{11},\chi_{12},\chi_{21},\chi_{22}\}$.

In our calculation, we neglect the heavy- and light-hole bands mixing and assume strictly parabolic dispersion relations. Also, the mixing of the exciton states by the Coulomb interaction is not taken into account because of its small effect on the narrow DQW system.[5] The $GaAs/Al_xGa_{1-x}As/AlAs$ material parameters and their compositional dependence is taken as in Refs. 1, 5, 9, and 10.

The χ_{ij}s are used to evaluate the optical oscillator strength (see, e.g., Ref. 4) and the electron-hole overlap integral $F_{ij}(0)$, which is given by

$$F_{ij}(0)=\int_{-\infty}^{\infty}\chi_{ij}(z_e=z,z_h=z,\rho=0)dz$$

$$=N_{ij}\int_{-\infty}^{\infty}\varphi_i^e(z)\varphi_j^h(z)dz. \quad (4)$$

The normalized exciton PL intensity spectrum is then calculated as

$$I(E)=\frac{\sum_{i,j=1}^{2}L_{ij}(E)|F_{ij}(0)|^2e^{-\beta E_{ij}}}{\sum_{i,j=1}^{2}|F_{ij}(0)|^2e^{-\beta E_{ij}}},$$

$$L_{ij}(E)=\frac{\beta\Delta_{ij}}{\pi}\int_0^\infty\frac{e^{-\beta E'}dE'}{(E-E_{ij}-E')^2+\Delta_{ij}^2}, \quad (5)$$

$\beta=1/k_BT$, k_B is the Boltzmann constant, and T the temperature. The convolution form $L_{ij}(E)$ expresses the normalized line shape of the i,jth transition, which is determined by a thermal distribution of the excitonic kinetic energy and slightly diffused by a Lorenz function. The width $\Delta_{ij}=0.5$ meV is used in every case.

III. EXPERIMENT

Our PL experiments were performed on a sample grown by molecular-beam epitaxy at a temperature of 600 °C on a semi-insulating GaAs substrate oriented in the [001] direction. The growth started with a 500 nm-wide n-doped (Si, 2×10^{18} cm^{-3}) GaAs layer, followed by a 300 nm-wide n-doped (Si, 1.4×10^{18} cm^{-3}) $Ga_xAl_{1-x}As$ layer. The Al content in the $Ga_xAl_{1-x}As$ layers was always 0.3. After this the following sequence of $Ga_xAl_{1-x}As$ layers was grown: 500-nm intrinsic, 5-nm p-δ-doped (C, 3×10^{17} cm^{-3}) layer, and 100-nm intrinsic. On top of this separating layer, a sequence of three symmetric DQW's with 4 ML (≈ 1.13 nm)-wide pure AlAs central barriers in between were grown, employing growth interruptions of 20 s at each heterointerface. The well widths are 35, 26, and 18 ML (≈ 10, 7.5, and 5 nm), respectively. The DQW's are separated by a 100 nm-wide $Ga_xAl_{1-x}As$ layer in each case. The growth then continued with another sequence of $Ga_xAl_{1-x}As$ layers: 100-nm intrinsic, 5-nm n-δ-doped (Si, 4×10^{17} cm^{-3}), and 500-nm intrinsic. On the top a 300 nm-wide p-doped (C, 1.4×10^{18} cm^{-3}) $Ga_xAl_{1-x}As$ layer and a 20 nm-wide p-doped (C, 2×10^{18} cm^{-3}) GaAs cap layer were grown.

The p-i-n configuration of the sample allows us to apply a bias voltage U_{pn} by means of selective Ohmic contacts to the p-doped layers on the top and to the n-doped layers at the bottom. Usually, the bands in any p-i-n structure are tilted and application of forward bias is required to flatten them. We, therefore, used a special sample design comprising δ-doped layers inside the intrinsic region of the structure in order to screen the built-in electric field. Thus, the flat-band

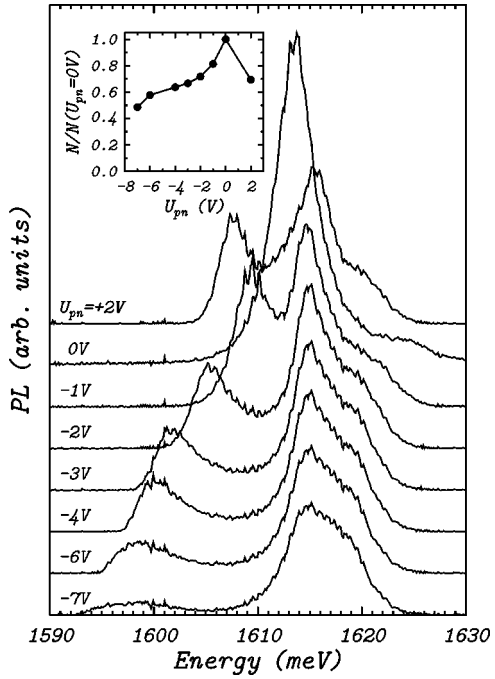

FIG. 2. PL spectra of the DQW with 5 nm-wide wells as a function of various bias voltages. The applied voltages U_{pn} are denoted beside each curve. The inset shows the normalized integral intensity $N/N(U_{pn}=0V)$ of the presented PL curves.

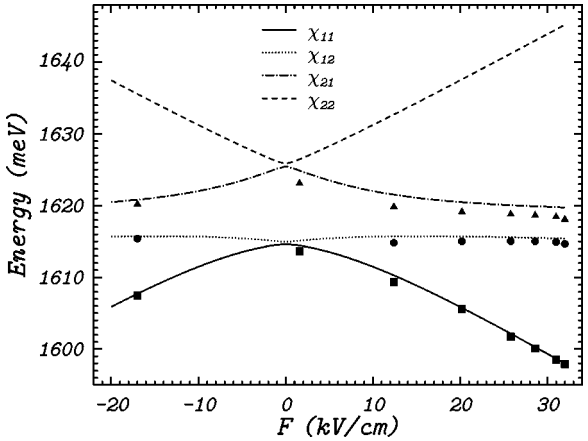

FIG. 3. PL peak positions as a function of electric field F. The lines are calculated for the DQW depicted in Fig. 1 at $T=45$ K. The markers indicate the peak positions of the experimental PL spectra plotted in Fig. 2.

regime is obtained almost at $U_{pn}=0$ V, avoiding high dark current present at higher forward bias. The measured devices of the size 250 μm$\times$250 μm were defined photolithographically and mesa-isolated. Detailed results will only be presented for the narrow DQW with $L_w=5$ nm and $L_b=1.13$ nm, for which the application of our simple theoretical model is justified.

Figure 2 shows the PL spectra of the sample for various bias voltages. The sample was cooled in a closed-cycle cryostat and excited by a Ti:sapphire laser pumped by an Ar^+-ion laser. We used an excitation power of ~ 100 mW/cm^2 at a photon energy of 1722 meV (below the band-gap energy of $Ga_{0.7}Al_{0.3}As$). The emitted luminescence was analyzed by a monochromator with 0.6 m focal length and a 1200 grooves/mm grating, and detected by a cooled charge coupled device camera. We applied reverse bias up to $U_{pn}=-8$ V with the maximum current of only ~ 10 μA. An estimation of a dissipated power and a negligible shift in position of the spectrum measured with $U_{pn}=+2$ V proved that Ohmic heating of the sample for both reverse and forward biased junction is insignificant.

IV. DISCUSSION

The sample was designed as a single (not multiple) DQW structure in order to minimize the well width fluctuations. For the same reason, the growth interruptions were employed, and a pure AlAs barrier instead of an $Al_xGa_{1-x}As$ one was chosen to improve its homogeneity and to avoid barrier height fluctuations. The broadening of the direct exciton peak of ~ 4 meV (see Fig. 2) and even lower at 10 K (~ 2 meV, not shown) indicates a quite good quality of the sample. Furthermore, the exciton peaks are not split due to large area monolayer fluctuations of the well widths, a phenomenon that is frequently observed on samples grown with interruptions.

The δ-doped layers shielding the DQW's within the p-n junction are effective in case of an excitation below the $Ga_{0.7}Al_{0.3}As$ band-gap energy, when the carriers are excited exclusively in the wells. The flat band condition is found almost at zero-bias voltage. On the other hand, when using a He-Ne laser excitation above band-gap energy, the δ-doped layers are neutralized and become inactive. Consequently, a forward bias corresponding to the band-gap energy is needed in order to overcome the built-in field and to establish the flat-band regime.

The experimental spectra plotted in Fig. 2 were analyzed to gain maximum data for the theoretical procedure. In the calculation, we kept the parameters L_w and L_b constant and varied only T and F for optimization. The temperature $T=45$ K of the sample was obtained by a comparison of the measured and calculated relative peak intensities of the spectra in the linear field range. The field F was deduced by means of tracing the energy distance between the first two exciton transitions χ_{11} and χ_{12}. A very good agreement of the calculated and observed transition energies is represented by Fig. 3. Notice that the optimized T provides an excellent correspondence in the peak positions. The absolute positions of all the peaks including the resonant splitting of the symmetric-antisymmetric states were obtained without any free parameter. The small difference in the intensities and positions of the theoretical lines ~ 1 meV in comparison with the experiment can be attributed to (i) the approximations used in the theory and (ii) small deviations from the intended structure of the sample.

The inset of Fig. 4 shows the deduced field F as a function of the bias voltage applied to the sample. In the case of the spectrum close to flat-band regime ($U_{pn}=0V$), the corresponding field ($F=1.6$ kV/cm) was determined from a linear part of this dependence. As anticipated, the dependence is linear within a limited voltage interval ($-3V \leq U_{pn} \leq 2V$), and saturates for higher reverse bias. The linear regime of the band tilting is in very good agreement with F calculated directly from the sample design (dotted line in

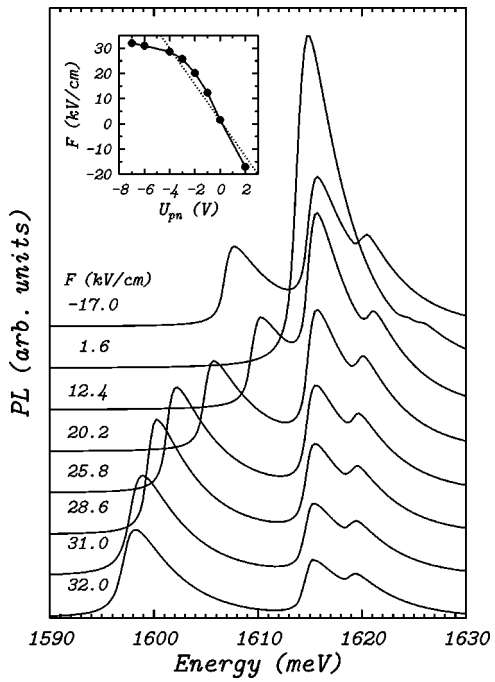

FIG. 4. Calculated PL spectra for the DQW depicted in Fig. 1 at a temperature $T=45$ K. The applied electric field F is given beside each curve. The inset shows the electric field induced in the DQW by the bias voltage U_{pn}.

the inset of Fig. 4). A small discrepancy can be explained as an effect of a nonhomogeneous distribution of the electric field over the three DQW systems, or as a result of a too simple description of the single wave functions in the applied variational method.

Figure 4 shows the spectra calculated for the studied DQW structure for the optimized temperature and the fields corresponding to individual PL curves plotted in Fig. 2. The spectra are magnified in accordance with the measured integral intensities $N(U_{pn})$ (see the inset of Fig. 2) to allow a comparison with the measured PL. The optimized temperature seems to be reasonable taking into account that the sample in a closed-cycle cryostat is cooled by a cold finger and placed on a rather low thermally conductive substrate. The close concert of the experimental and calculated PL spectra in the low-field interval $(-3V \leqslant U_{pn} \leqslant 2V)$ is evident. By increasing reverse bias the observed indirect transition diminishes. This results from a low stability of the lowest energy χ_{11} exciton, which becomes dissociated by electron tunneling outside the DQW. The highest transition χ_{22} appears near the flat-band case only. It manifests itself in Fig. 4 in the spectrum calculated for $F=1.6$ kV/cm as the small peak at the energy of 1626 meV close to the χ_{21} transition. In the experiment, these transitions merge into one peak observed at 1623 meV. Out of the flat-band case, χ_{22} is suppressed due to a weak population of the higher levels and the lower value of the electron-hole overlap integral $F_{22}(0)$ [Eq. (4)]. With respect to the good agreement of relative intensities of the spatially direct and indirect transitions we can conclude that the overlap integrals are well estimated and the particle distribution is described by our wave functions in a satisfactory way.

V. CONCLUSION

In this paper, we have concentrated on the photoluminescence of narrow symmetric coupled double quantum wells, where the energy difference between excitonic states is high enough to allow neglecting of band-mixing effects. The inclusion of exciton interaction is unavoidable for a correct description of the electron-hole states and positioning of optical transitions. We have shown that the simple model describes nearly perfectly all dominant features of the optical transitions, namely relative intensities, absolute positions of the individual transitions, and the resonant splitting of the symmetric-antisymmetric states.

ACKNOWLEDGMENTS

This work was supported by the Friedrich-Alexander-Universität Erlangen-Nürnberg, by the Grant Agency of the Czech Republic (Grant Nos. 202/95/1533 and 202/98/0085), and by the Ministry of Education of the Czech Republic (Grant No. VS-97113). R. Grill acknowledges support from the Alexander von Humboldt Foundation (AvH, Bonn, Germany).

*Electronic address: soubusta@alma.karlov.mff.cuni.cz

[1] G. Bastard, *Wave Mechanics Applied to Semiconductor Heterostructures* (Monographies de physique, Paris, 1992).
[2] C. Weisbuch and B. Winter, *Quantum Semiconductor Structures* (Academic Press, New York, 1991).
[3] J. Lee, M. O. Vassell, E. S. Koteles, and B. Elman, Phys. Rev. B **39**, 10 133 (1989).
[4] M. M. Dignam and J. E. Sipe, Phys. Rev. B **43**, 4084 (1991).
[5] T. Westgaard, Q. X. Zhao, B. O. Fimland, K. Johannessen, and L. Johnsen, Phys. Rev. B **45**, 1784 (1992).
[6] Y. Takahashi, Y. Kato, S. S. Kano, S. Fukatsu, Y. Shiraki, and R. Ito, J. Appl. Phys. **76**, 2299 (1994).
[7] M. Bayer, V. B. Timofeev, F. Faller, T. Gutbrod, and A. Forchel, Phys. Rev. B **54**, 8799 (1996).
[8] A. V. Akimov, E. S. Moskalenko, A. L. Zhmodikov, D. A. Mazurenko, A. A. Kaplyanskii, L. J. Challis, T. S. Cheng, and C. T. Foxon, Fiz. Tverd. Tela **39**, 735 (1997) [Sov. Phys. Solid State **39**, 649 (1997)].
[9] K. K. Bajaj, in *Properties of III-V Quantum Wells and Superlattices*, edited by P. Bhattacharya (INSPEC, London, 1996), No. 15, p. 55.
[10] R. Pässler and G. Oelgart, J. Appl. Phys. **82**, 2611 (1997).